Tanzania Journal of Science
Volume 51(4), 2025
journal homepage: https://commons.udsm.ac.tz/tjs/

Simulation based model for canine distemper virus in prey-predator dynamics

Mussa A. Stephano*
Department of Mathematics, Physics and Informatics,
University of Dar es Salaam, Mkwawa University College of Education, P.O. Box 2513,
Iringa, Tanzania.

Keywords

Canine Distemper Virus;
Prey-Predator;
Monte Carlo Simulations;
Basic Reproduction Number

Abstract

This study investigates the dynamic interactions of a prey-predator ecosystem infected with Canine Distemper Virus (CDV), focusing on predation and disease transmission. A deterministic model, coupled with Monte Carlo simulations (MCS), employed to capture both stochastic variability and environmental fluctuations. The findings indicate that classical prey-predator cycles provide the baseline for population dynamics, but the introduction of CDV and environmental noise fundamentally alters system behavior. Initially, populations exhibit oscillations that gradually stabilize into dynamic equilibria. However, the disease persists within both prey and predator populations, suggesting endemicity rather than extinction. Predation plays a dual role in disease dynamics, while it reduces prey abundance and can limit pathogen spread, it also exposes predators to infection through consumption of infected prey, thereby generating nonlinear feedbacks that affect population stability. Infection affects ecological linkages, diminishes predator viability, and increases volatility in interspecies interaction, as reflected in phase-space trajectories and weak correlations among population classes. These findings emphasize the critical interplay between predation, disease, and stochasticity in shaping long-term ecological outcomes and highlight the importance of integrating these factors into ecological models for accurate prediction of disease persistence and extinction risk.

Introduction

Canine Distemper Virus (CDV) is a highly contagious, multi-host pathogen that poses a significant threat to domestic and wild carnivore populations globally (Naveenkumar et al. 2020). CDV is caused by a single-stranded RNA virus belonging to the genus *Morbillivirus* in the family *Paramyxoviridae* (Niewiesk and Oglesbee 2022). The CDV primarily infects domestic dogs, which often serve as a host for transmission to diverse wildlife species (Martinez-Gutierrez and Ruiz-Saenz 2016). The spread of CDV occurs mainly through aerosol droplets, direct contact with infected bodily fluids and contaminated environments in animal's habitat (Deem et al. 2000). The infected animals typically exhibit a wide spectrum of clinical symptoms, including respiratory distress, gastrointestinal complications, and severe neurological manifestations (Sykes and Vandevelde 2021). Figure 1 illustrates some common physical symptoms of CDV in both prey and predator. Moreover, the mortality rates can be exceedingly high, especially among wildlife populations when the treatment is not implemented (De Risio and Platt 2014).

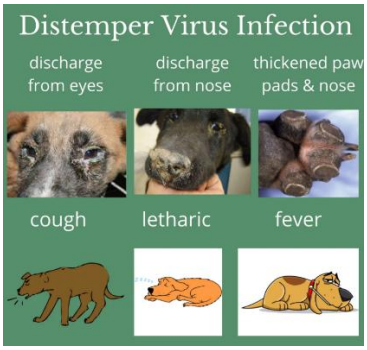

Figure 1: Symptoms of Canine Distemper Virus infection on prey and predator (Sykes and Vandevelde 2021).

*Corresponding author: mussaamos314@gmail.com; mussa.amos@muce.ac.tz
Received 20 July 2025; Revised 14 Nov 2025; Accepted 22 December 2025; Published 29 December 2025
https://doi.org/10.65085/2507-7961.1113

ISSN 0856-1761, e-ISSN 2507-7961

Globally, CDV outbreaks have been reported on nearly every continent, causing substantial conservation and economic burdens (Wipf et al. 2025). Serengeti epidemic led to the death of approximately one-third of the lion population, highlighting the devastating potential to vulnerable wildlife (Pomeroy-Arthur 2023). Despite ongoing vaccination campaigns for domestic dogs, the persistence and spread of CDV in wild populations emphasize the challenge of managing multi-host pathogens in prey and predator interactions. The burden of CDV transcends ecological impacts, as outbreaks disrupt prey-predator dynamics, reduce biodiversity, and complicate conservation efforts for threatened species. Predicting the spread and impact of CDV under varying ecological and climatic conditions remains a pressing need.

Compartmental models have been employed to simulate Canine Distemper Virus (CDV) dynamics in both domestic and wild populations (Viana et al. 2015, White et al. 2018, Hayes et al. 2023, Rendon-Marin and Ruíz-Saenz 2024). These models have provided valuable insights into disease transmission, host susceptibility, and outbreak potential. However, the reliability of such models is often constrained by parameter uncertainty arising from limited field data and by the complex, stochastic nature of wild interactions which can lead to significant deviations from predicted outcomes.
For instance, outbreaks of CDV have been documented in African lions (*Panthera leo*) following infection in prey populations such as the African wild dog (*Lycaon pictus*) (Viana et al. 2015). Similarly, interactions between foxes and small rodent populations in Europe have been associated with local CDV spillover events (White et al. 2018). These cases demonstrate the ecological relevance of studying prey-predator disease dynamics.

Monte Carlo simulation (MCS) offers a promising approach to address these challenges by incorporating both parameter estimation and stochastic variability into disease models. Unlike deterministic models, which produce single point estimates, MCS generates probabilistic outcomes that capture the range of possible epidemic trajectories under fluctuating environmental and host population conditions (Santoro et al. 2024, Chen et al. 2025). This is particularly relevant for rare spillover events, multi-host interactions, and ecological contexts where prey-predator relationships modulate infection spread.

The CDV can be transmitted through bodily fluids, excretions, or carcasses, which can contaminate shared habitats, water sources, or feeding grounds, thereby facilitating indirect transmission among susceptible hosts (Hayes et al. 2023). This environmental dimension is essential for understanding the persistence of the virus in ecosystems and the role of predation in disease simulation.

Despite that MCS potentials, few studies have integrated MCS with ecological and epidemiological modeling in multi-host prey-predator system. In these systems, indirect interactions and cascading trophic effects can profoundly influence both the prevalence and persistence of infections, yet these dynamics remain largely unexplored. For example, predation on infected prey can either suppress or amplify disease spread depending on predator selectivity and prey susceptibility, creating nonlinear feeding loops that deterministic models alone cannot capture.

This gap emphasizes the need for modeling frameworks that explicitly couple random simulations with ecological and epidemiological parameters enabling more robust assessment of disease risk, transmission pathways. This study develops a comprehensive deterministic model of CDV transmission within prey-predator ecosystems, enhanced with Monte Carlo simulations to capture ecological variability and stochastic effects. By linking predation dynamics with infection process, the model aims to provide new insights into how CDV propagates through trophic interactions and how stochastic forces shape population persistence, extinction risk, and ecosystem resilience.

Therefore, this work addresses a critical methodological gap in disease ecology by integrating deterministic model and Monte Carlo simulation, offering a framework that can inform both theoretical understanding and practical management of wildlife diseases.

Model Formulation

In this study, a deterministic mathematical model to describe the dynamics of prey and predator populations, incorporating the effects of Canine Distemper Virus (CDV) was formulated. The model considers four interacting subpopulations: susceptible prey $S_1(t)$, infected prey $I_1(t)$, susceptible predators (t) and infected predators $I_2(t)$. It is assumed that, in the absence of predators and disease, the prey population grows logistically with an intrinsic growth rate r and an environmental carrying capacity C. Predators feed on both susceptible and infected prey at rates and α_2, respectively, and their growth depends on the biomass gained through predation, with biomass conversion efficiencies ψ_1 and ψ_2 corresponding to susceptible and infected prey (Stephano and Jung 2021). It is assumed that, because predator population growth relies on biomass derived from the prey population, its dynamics deviate from the conventional logistic growth formulation. Disease transmission occurs through direct contact within each species: susceptible prey $S_1(t)$ become infected by interacting with infected prey $I_1(t)$ at a rate β, while susceptible predators $S_2(t)$ contract the disease through contact with infected predators $I_1(t)$ at a rate χ. Infected individuals, both prey and predators, experience natural mortality at a rate μ as well as additional disease-induced mortality at a rate δ in both prey and predator populations. The model assumes a homogeneous environment where individuals mix uniformly (Valdez et al. 2025), resulting in random interactions for predation and infection, no migration, no recovery or immunity from infection, and relatively constant ecological parameters over time. The model further assumes that infection occurs through both direct and indirect pathways, irrespective of the source, such as host contact or exposure to a contaminated environment.

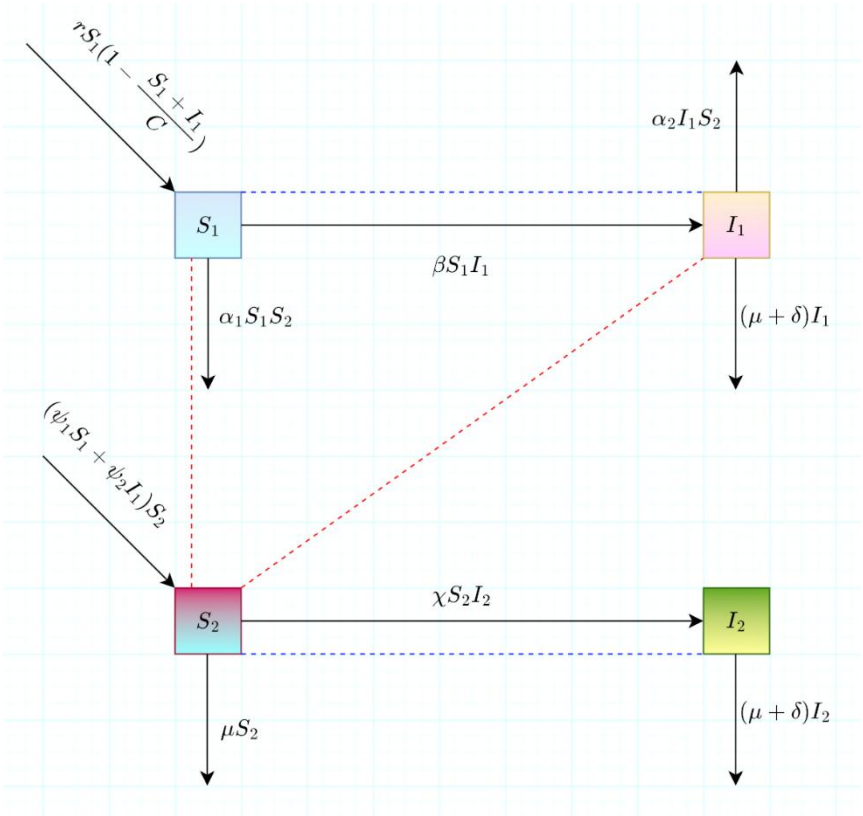

Figure 2: The model flow diagram for population dynamics of predator and prey with CDV infection

The model for dynamics predator and prey with CDV infection is given by the system (1):

$$\begin{aligned}
\frac{dS_1}{dt} &= rS_1 - \frac{rS_1(S_1+I_1)}{C} - \alpha_1 S_1 S_2 - \beta S_1 I_1,\\
\frac{dI_1}{dt} &= \beta S_1 I_1 - \alpha_2 I_1 S_2 - (\mu+\delta) I_1,\\
\frac{dS_2}{dt} &= \psi_1 S_1 S_2 + \psi_2 I_1 S_2 - \chi S_2 I_2 - \mu S_2,\\
\frac{dI_2}{dt} &= \chi S_2 I_2 - (\mu+\delta) I_2.
\end{aligned} \tag{1}$$

Subject to the following initial conditions: $S_1(0) > 0; I_1(0) \geq 0; S_2(0) > 0; I_2(0) \geq 0.$

Model Analysis

This section demonstrates that the model solutions are well-posed, positive and bounded.

Positivity of Model Solutions

The analysis of non-negativity for the model system (1) is performed to give

$$\begin{aligned}
S_1(t) &\geq S_1(0) e^{-\int_0^t \left(\frac{r}{C}(S_1(\tau)+I_1(\tau)+\alpha_1 S_2(\tau)+\beta I_1(\tau))\right) d\tau} \geq 0,\\
I_1(t) &\geq I_1(0) e^{-\int_0^t (\alpha_2 S_2(\tau)+\mu+\delta)\, d\tau} \geq 0,\\
S_2(t) &\geq S_2(0) e^{-\int_0^t (\chi I_2(\tau)+\mu)\, d\tau} \geq 0,\\
I_2(t) &\geq I_2(0) e^{-(\mu+\delta)t} \geq 0.
\end{aligned}$$

Therefore, all model solutions are non-negative for all t > 0.

Existence of Model Solutions

With the initial conditions, the model solution is non-negative, in this section, we use the Lipschitz condition to show existence of the model solution.

$$S_1(t) - S_1(0) = \int_0^t \left(rS_1 - \frac{rS_1(S_1+I_1)}{C} - \alpha_1 S_1 S_2 - \beta S_1 I_1\right) d\tau$$

$$
\begin{aligned}
I_1(t) - I_1(0) &= \int_0^t (\beta S_1 I_1 \ - \alpha_2 I_1 S_2 - (\mu + \delta) I_1)\, d\tau, \\
S_2(t) - S_2(0) &= \int_0^t (\psi_1 S_1 S_2 + \psi_2 I_1 S_2 - \chi S_2 I_2 - \mu S_2)\, d\tau, \\
S_2(t) - S_2(0) &= \int_0^t (\chi S_2 I_2 - (\mu + \delta) I_2)\, d\tau,
\end{aligned} \tag{2}
$$

For convenience, equation (2) is defined by the following kernel

$$
\begin{aligned}
k_1(t, S_1) &= rS_1 - \tfrac{rS_1(S_1 + I_1)}{C} - \alpha_1 S_1 S_2 - \beta S_1 I_1, \\
k_2(t, I_1) &= \beta S_1 I_1 \ - \alpha_2 I_1 S_2 - (\mu + \delta) I_1, \\
k_3(t, S_2) &= \psi_1 S_1 S_2 + \psi_2 I_1 S_2 - \chi S_2 I_2 - \mu S_2, \\
k_4(t, I_2) &= \chi S_2 I_2 - (\mu + \delta) I_2.
\end{aligned} \tag{3}
$$

Since, $S_1,\ I_1, S_2, I_2$ are positive and bounded, there exists non-negative $\omega_j, j = 1, 2, 3, 4$. Such that $\big||S_1(t)|\big| \leq\ \omega_1$, $\big||I_1(t)|\big| \leq\ \omega_2$, $\big||S_2(t)|\big| \leq\ \omega_3$, and $\big||I_2(t)|\big| \leq\ \omega_4$,

By defining arbitrary function gives:

$$
\begin{aligned}
&||k_1(t, S_1) - k_1(t, S_{1^*}(t))|| \leq (r\omega_1 - \frac{1}{C} - \alpha_1\omega_3 - \beta\omega_2)||S_1 - S_{1^*}||, \\
&||k_2(t, I_1) - k_2(t, I_{1^*}(t))|| \leq (\beta\omega_1 - \alpha_2\omega_3 - \mu - \delta)||I_1 - I_{1^*}||, \\
&||k_3(t, S_2) - k_3(t, S_{2^*}(t))|| \leq (\psi_1\omega_1 + \psi_2\omega_2 - \chi\omega_4 - \mu)||S_2 - S_{2^*}||, \\
&||k_4(t, I_2) - k_4(t, I_{2^*}(t))|| \leq (\chi\omega_3 - \mu - \delta)||I_2 - I_{2^*}||.
\end{aligned}
$$

Since, the Lipschitz condition is satisfied, the model solutions of the model exist and convergent (Stephano et al. 2024).

CDV free equilibrium point E^0 and Reproduction Number $\mathcal{R}_0$

When there is no infection in predator and prey populations, gives the disease-free state E^0 as

$$E^0 = \left(\frac{\mu}{\psi_1}, 0, \frac{r}{\alpha_1} - \frac{r\mu}{C\alpha_1\psi_1}, 0\right).$$

The secondary infection resulting from one infected individual in a completely susceptible population is referred as basic reproduction number $\mathcal{R}_0$(Stephano et al. 2023). The value $\mathcal{R}_0 < 1$ and $\mathcal{R}_0 \geq 1$ represents extinction and persistence of CDV infection, respectively (Clancy and Tjia 2018, Yan et al. 2016). The next generation matrix approach used to compute a basic reproduction number $\mathcal{R}_0$ as follows:

The system (1) decomposed to form the vectors for new infections $\mathcal{F}_j$ and transfer terms $\mathcal{L}_i$ to form:

$$\mathcal{F}_j = \begin{pmatrix} \beta S_1 I_1 \\ \chi S_2 I_2 \end{pmatrix},\ \mathcal{L}_i = \begin{pmatrix} \alpha_2 I_1 S_2 + (\mu + \delta) I_1 \\ (\mu + \delta) I_2 \end{pmatrix}. \tag{4}$$

Matrices $\mathcal{F}_i$ and $\mathcal{L}_i$ are defined by:

$$\mathcal{F}_i = \frac{\partial F_i}{\partial X_j}(E^0),\ \mathcal{L}_i = \frac{\partial V_i}{\partial X_J}(E^0), \tag{5}$$

The spectral radius of the matrix $\mathcal{F}\mathcal{L}^{-1}$ is the basic reproduction number denoted by $\mathcal{R}_0$ as

$$\mathcal{R}_0 = \rho(\mathcal{F}\mathcal{L}^{-1})\,. \tag{6}$$

Applying the definition in equation (6), we obtain:

$$\mathcal{R}_0 = \frac{\beta\mu}{\mu\alpha_2 + \psi_1(\mu + \delta)} \tag{7}$$

The Endemic Equilibrium (E^*)

In the presence of CDV infections in both predator and prey population, give endemic equilibrium point $E^* = (S_1^*, I_1^*, S_2^*, I_2^*)$ where:

$$S_1^* = \frac{\alpha_2(\mu + \delta)}{\chi} + \mu + \delta,\ I_1^* = \frac{C}{\beta C + r}\left(r - \frac{rS_1^*}{C} - \alpha_1 S_2^*\right),\ S_2^* = \frac{\mu + \delta}{\chi},\ I_2^* = \frac{1}{\chi}(\psi_1 S_1^* + \psi_2 I_1^* - \mu)$$

Stability Analysis of E^0

The Metzler matrix approach was employed to assess the global stability of the CDV-free equilibrium. System (1) was decomposed into two matrices: S representing the non-infectious classes, and I representing the infectious classes. The decomposition is defined as follows:

$$S = \begin{pmatrix} S_1 \\ S_2 \end{pmatrix}, I = \begin{pmatrix} I_1 \\ I_2 \end{pmatrix} \text{ and } S - E^0 = \begin{pmatrix} S_1 - \frac{\mu}{\psi_1} \\ S_2 + \frac{r\mu}{C\alpha_1\psi_1} - \frac{r}{\alpha_1} \end{pmatrix}$$

$$\frac{dS}{dt} = A(S - E^0) + DI$$

$$\frac{dI}{dt} = BI.$$

The eigenvalues of the matrix A are negative and off-diagonal element of the matrix B are non-negative, following the properties of Metzler matrix, then E^0 is globally asymptotically stable.

Stability Analysis of E^*

The global stability of the endemic equilibrium point is established using a Lyapunov function approach. Specifically, the Lyapunov function is constructed and defined as follows:

$$L = S_1^*\left(\frac{S_1}{S_1^*} - \ln\frac{S_1}{S_1^*}\right) + I_1^*\left(\frac{I_1}{I_1^*} - \ln\frac{I_1}{I_1^*}\right) + S_2^*\left(\frac{S_2}{S_2^*} - \ln\frac{S_2}{S_2^*}\right) + I_2^*\left(\frac{I_2}{I_2^*} - \ln\frac{I_2}{I_2^*}\right)$$

Differentiating throughout gives;

$$\frac{dL}{dt} = \left(1 - \frac{S_1^*}{S_1}\right)\frac{dS_1}{dt} + \left(1 - \frac{I_1^*}{I_1}\right)\frac{dI_1}{dt} + \left(1 - \frac{S_2^*}{S_2}\right)\frac{dS_2}{dt} + \left(1 - \frac{I_2^*}{I_2}\right)\frac{dI_2}{dt}$$

Direct substitution into the equation yields;

$$\frac{dL}{dt} = \left(1 - \frac{S_1^*}{S_1}\right)\left(rS_1 - \frac{rS_1(S_1 + I_1)}{C} - \alpha_1 S_1 S_2 - \beta S_1 I_1\right) + \left(1 - \frac{I_1^*}{I_1}\right)(\beta S_1 I_1 - \alpha_2 I_1 S_2 - (\mu + \delta)I_1)$$
$$+ \left(1 - \frac{S_2^*}{S_2}\right)(\psi_1 S_1 S_2 + \psi_2 I_1 S_2 - \chi S_2 I_2 - \mu S_2) + \left(1 - \frac{I_2^*}{I_2}\right)(\chi S_2 I_2 - (\mu + \delta)I_2)$$

$$M = rS_1 + rS_1^*\left(\frac{S_1 + I_1}{C}\right) + \alpha_1 S_1^* S_2 + \beta S_1^* I_1 + \beta S_1 I_1 + \alpha_2 I_1^* S_2 + (\mu + \delta)I_1^* + \psi_1 S_1 S_2 + \psi_2 I_1 S_2 + \chi S_2^* I_2 + \chi S_2 I_2 + (\mu + \delta)I_2^*$$

$$N = rS_1^* + rS_1\left(\frac{S_1 + I_1}{C}\right) + \alpha_1 S_1 S_2 + \beta S_1 I_1 + \alpha_2 I_1 S_2 + (\mu + \delta)I_1 + \beta I_1 I_1^* + \psi_1 S_1 S_2^* + \psi_2 I_1 S_2^* + \chi S_2 I_2 + \chi S_2 I_2^* + \mu(S_2 + S_2^*) + (\mu + \delta)I_2$$

$$\frac{dL}{dt} = M - N$$

If $M < N$ then $\frac{dL}{dt} < 0$, as $t \to \infty$, the solution of the system (1) approaches the endemic equilibrium point E^* when $\mathcal{R}_0 > 1$. Therefore, E^* is globally asymptotically stable in the bounded region, otherwise unstable.

Numerical Simulation

In this work, Monte Carlo simulation is used alongside ordinary differential equations (ODEs) in prey-predator models to incorporate the inherent randomness and uncertainty present in ecological systems. While ODEs provide a deterministic framework describing the average behavior of predator and prey populations based on biological interactions, real ecosystems are influenced by unpredictable environmental fluctuations, random events, and parameter variability (Sadiq 2025). By running the ODE model multiple times with parameters and initial conditions randomly sampled from probability distributions, Monte Carlo simulation captures a wide range of possible outcomes rather than a single fixed trajectory (Shetty et al. 2024). This approach provides assess how uncertainties in parameters like predation rates or disease transmission affect population dynamics, explore the stability and resilience of the system, and provide probabilistic insights that improve the robustness and realism of model predictions. The initial values used in the simulations were chosen arbitrarily, as the system demonstrated stability and convergence under the applied numerical method. This indicates that the model's qualitative behavior is not sensitive to small variations in initial conditions. Integrating Monte Carlo simulations with ordinary differential equations (ODEs) therefore provides a powerful framework to explore and manage complex prey-predator interactions under natural variability. The model system (1) was simulated based on the following initials $S_1(0) = 30$, $S_2(0) = 20$, $I_1(0) = 1$, $I_2(0) = 1$ and parameter values described in Table 1.

Table 1. Parameter values

Parameter	Description	Value (per month)	Citation
r	Intrinsic growth rate	0.3000	Stephano and Jung, 2021
β	Prey infection rate	0.0300	Rendon-Marin and Ruiz-Saenz, 2024
α_1	Predator feed susceptible prey rate	0.0250	Stephano and Jung, 2021
α_2	Predator feed infected prey rate	0.0750	Hayes et al., 2023
ψ_1	Biomass conversion rate from susceptible prey	0.0200	White et al., 2018
ψ_2	Biomass conversion rate from infected prey	0.0025	Viana et al., 2015
χ	Predator infection rate	0.0300	Santoro et al., 2024
μ	Natural mortality at a rate	0.0045	Dorn and Barnes, 2022
δ	Induced death rate	0.0005	Chen et al., 2025
C	Carrying capacity	300.00	Hayward et al, 2007

Figure 3, illustrates prey-predator population dynamics both in the absence and presence of environmental noise, presented across four distinct panels. 3(a) shows the healthy prey population, where the solid blue line represents the deterministic model with regular oscillations characteristic of natural prey-predator cycles. When environmental noise is introduced, indicated by the shaded blue area with a dashed line, fluctuations appear around this pattern, causing irregular peaks and dips. 3(b) depicts the infected prey population; here, noise similarly induces unpredictable spikes and drops, highlighting how random factors can influence disease prevalence within prey. 3(c) presents the healthy predator population, which cycles smoothly without noise but exhibits erratic fluctuations under stochastic conditions, sometimes nearing extinction or surging unexpectedly. 3(d) displays the infected predator population, where noise similarly increases variability, resulting in sudden outbreaks or declines.

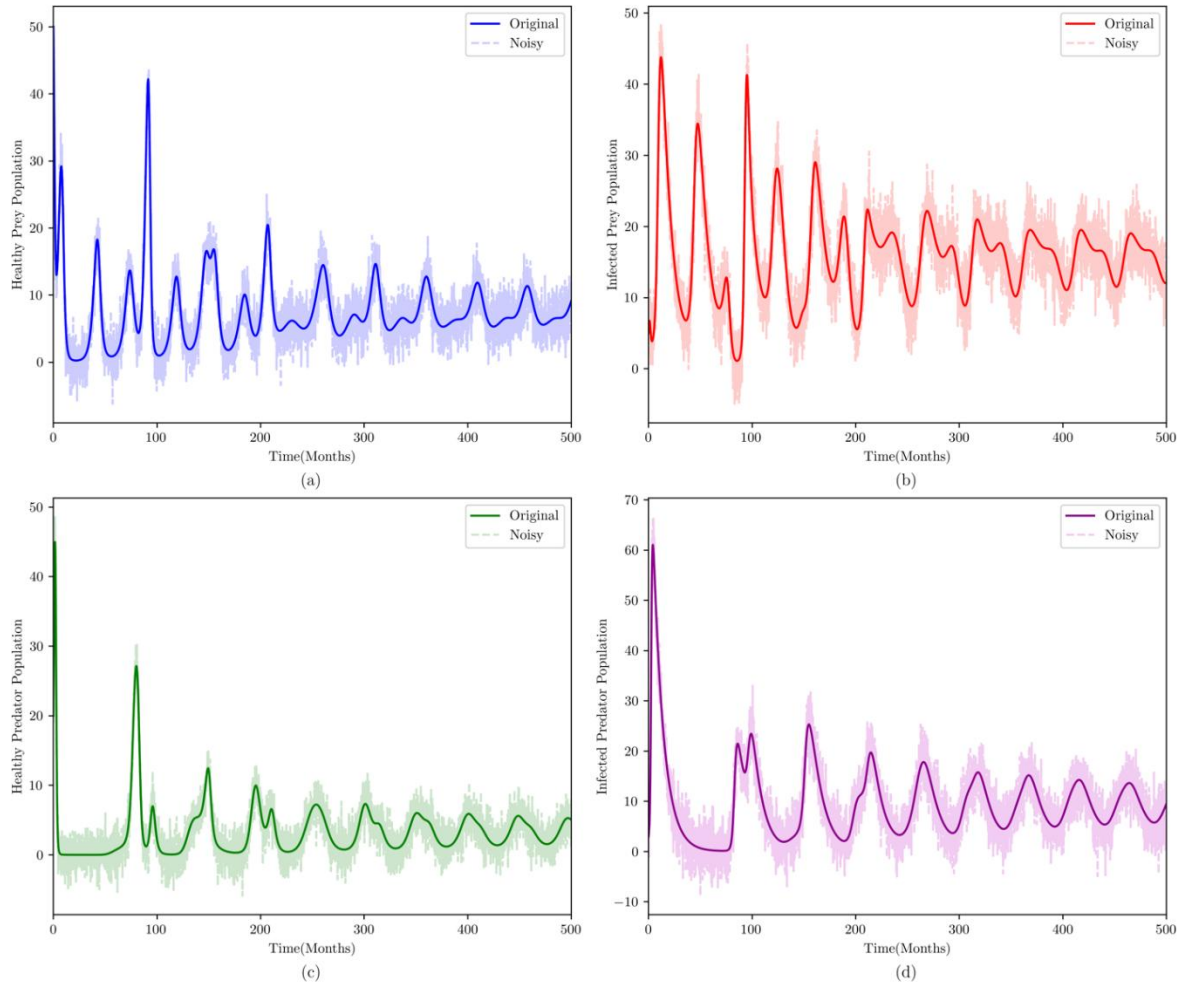

Figure 3: Dynamics of Predator and prey populations

Figure 4, presents time series plots illustrating the population dynamics of four distinct groups healthy prey, infected prey, healthy predators, and infected predators at four time points: 100, 200, 300, and 400 months. Each row corresponds to one of these time points, while each column represents a specific population group. The healthy prey population demonstrates oscillatory behavior with peaks and troughs that gradually stabilize into smaller fluctuations, reflecting natural cycles of growth and decline influenced by predation and ecological factors. The infected prey population also oscillates but maintains generally lower sizes, with repeated peaks indicating disease outbreaks that tend to diminish in amplitude over time, suggesting a move toward endemic equilibrium. Healthy predators exhibit sharp rises and falls early on, which become more frequent and moderate as time progresses, indicating a dynamic balance with prey populations. Infected predators start at higher levels and fluctuate with repeated peaks that slowly decrease, possibly due to disease control or predator mortality.

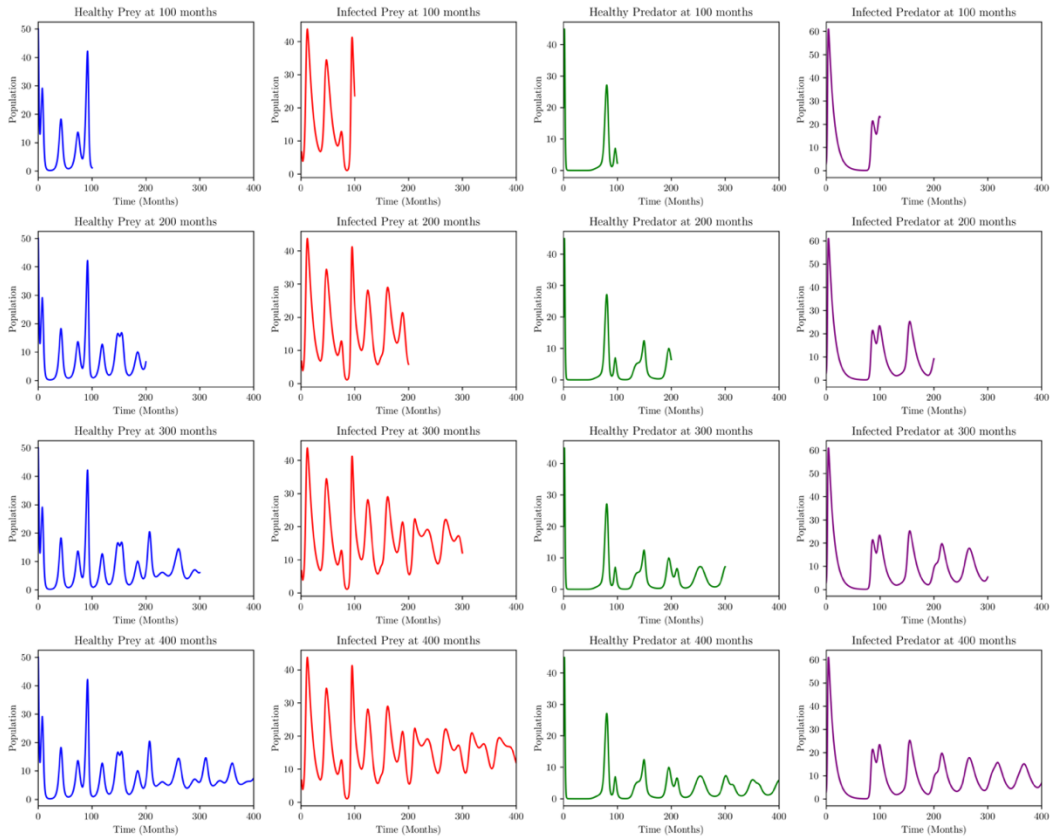

Figure 4: The population dynamics of four distinct groups healthy prey, infected prey, healthy predators, and infected predators at 100, 200, 300, and 400 months.

Figure 5(a), the Healthy Prey population exhibits significant initial fluctuations, likely driven by both predation and infection pressure. However, as time progresses, these oscillations decrease, and the population stabilizes at a moderate level, indicating the system's tendency toward equilibrium. Figure 5(b) shows the Infected Prey population, which similarly undergoes large fluctuations early on but stabilizes over time at a level slightly higher than the healthy prey. This suggests that the disease persists within the prey population and becomes endemic rather than being eradicated. Figure 5(c), the Healthy Predator population initially increases but then rapidly declines, with the mean stabilizing at a low value. This may be due to reduced availability of healthy prey or the impact of infection within the predator population. Figure 5(d) shows that the Infected Predator population also fluctuates strongly at first, reaching high peaks in some runs, but ultimately stabilizes at a relatively high average population, reinforcing the idea of disease persistence among predators as well.

The findings show the following key insights: (i) all four population types tend toward stable mean values over time despite early volatility, indicating a degree of long-term stability or resilience in the ecosystem. (ii) both infected prey and predators maintain substantial populations in the steady state, pointing to the persistence of disease within the system. This highlights the challenge of eradicating infections once they become endemic. (iii) the consistently low number of healthy predators suggests that predator health may be highly sensitive to the availability of healthy prey, which itself is constrained by the spread of disease. (iv) the contrast between the healthy and infected populations in both prey and predator groups underlines the importance of disease dynamics in shaping population structures. These simulations emphasize the interconnected roles of infection and predation in determining ecological stability and population balance.

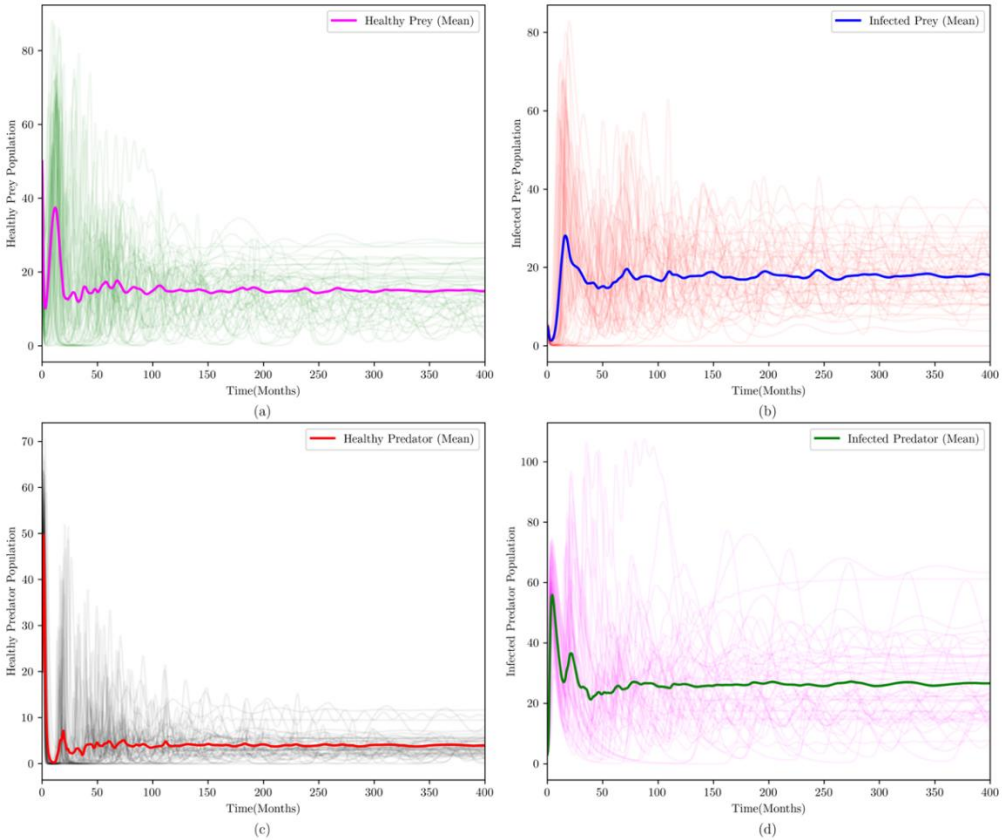

Figure 5: Monte Carlo Simulation of prey-predator model system, presenting the dynamics of the populations in each compartment.

Figure 6(a), which shows the relationship between healthy prey and healthy predators, the trajectories form closed or spiraling loops, indicative of classic prey-predator cycles. As the healthy prey population increases, the healthy predator population also rises due to increased food availability. However, once predator numbers peak, they reduce the prey population, eventually leading to a decline in predators due to food scarcity. These oscillations gradually dampen, suggesting the system trends toward a stable equilibrium over time. Figure 6(b) explores the interaction between healthy prey and infected predators. Unlike the more orderly loops in 5(a), this plot shows a wider spread and more complex trajectories, indicating less direct and more nonlinear dynamics. While infected predator populations might indirectly benefit from higher prey numbers, the relationship is inconsistent, likely due to the compounding effects of disease, reduced hunting efficiency, or increased mortality among infected predators. Figure 6(c), the dynamics between infected prey and healthy predators are displayed. Here, the patterns also show spiraling behavior, but with more asymmetry and dispersion, suggesting a weaker or more variable relationship. This may result from healthy predators avoiding infected prey or being less successful in preying on them. Consequently, fluctuations in the infected prey population do not consistently support the growth of the healthy predator population, indicating a potential destabilizing influence of disease on this interaction. Figure 6(d) highlights the relationship between infected prey and infected predators. This plot exhibits the most complex and overlapping trajectories, pointing to strong coupling between these two infected groups. The patterns suggest chaotic or multi-phase dynamics, with the populations fluctuating in response to each other in a tightly linked, yet unpredictable, manner. Nevertheless, the overall distribution of points appears bounded, hinting at a long-term persistence of disease within the ecosystem rather than extinction.

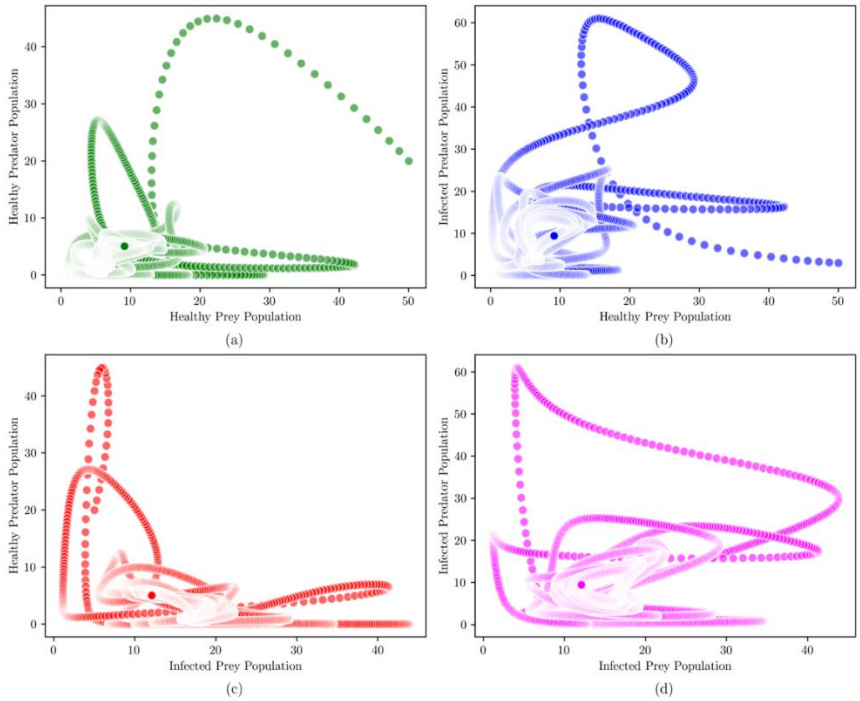

Figure 6: The dynamic interactions between pairs of populations within the ecosystem.

Figure 7, Shows the correlation matrix of population dynamics illustrates the relationships between healthy prey, infected prey, healthy predator, and infected predator. The diagonal elements all have a value of 1, as each variable is perfectly correlated with itself. Among the off-diagonal elements, several weak to moderate correlations emerge. Healthy Prey shows a weak positive correlation with both healthy predator of 0.29 and infected predator of 0.34, suggesting that healthy prey may support the populations of both predator types to some extent. Conversely, healthy prey is weakly negatively correlated with infected prey of -0.25, which could indicate that as disease spreads within the prey population, the number of healthy individuals declines. infected prey also shows a moderate negative correlation with healthy predator of -0.39, potentially implying that predators prefer or are more successful in capturing healthy rather than infected prey. Meanwhile, the correlation between infected prey and infected predator is weakly positive of 0.16, hinting at a slight synchrony in their dynamics, possibly due to shared environmental or biological factors. Interestingly, there is virtually no correlation between healthy and infected predators of -0.0094, suggesting that the health states of predators may fluctuate independently. Overall, the matrix highlights subtle but important interactions in the population dynamics driven by health status and predation.

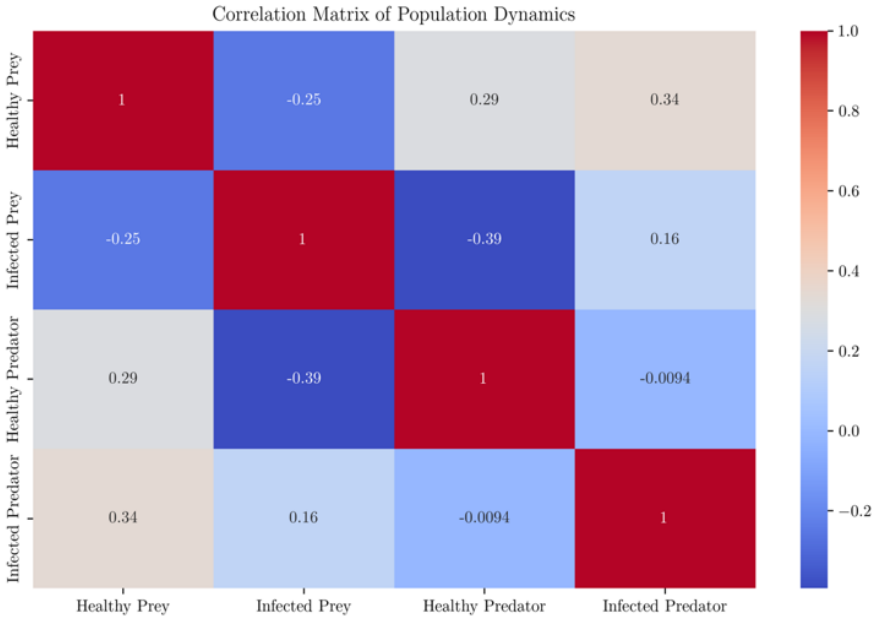

Figure 7: The correlation matrix of population dynamics illustrates the relationships between healthy prey, infected prey, healthy predator, and infected predator.

Discussion

The results demonstrate that stochastic perturbations substantially increase variability around deterministic prey-predator dynamics, leading to amplified fluctuations in both healthy and infected populations. This increased dispersion increases outbreak risk and changes population baselines, indicating that purely deterministic models may underestimate extinction risk endemic states. These findings are consistent with the observations by White et al. (2018), that emphasized on environmental randomness and nonlinear transmission processes fundamentally alter wildlife disease dynamics. In contrast to stabilizing mechanisms such as prey refuge reported by Stephano and Jung (2021). This study shows that stochasticity coupled with disease transmission can destabilize classical prey-predator systems, reinforcing the need to move beyond deterministic models.

The persistence of infection at non-zero levels in both prey and predator populations highlights the emergence of endemic states even when the system dynamics stabilize. This finding aligns with the empirical evidence of sustained CDV circulation across multiple host species reported by Martínez-Gutiérrez and Ruiz-Saenz (2016). This model extends these findings by providing a mechanistic explanation, demonstrating how predation-mediated transmission and stochastic environmental effects jointly maintain infection. Such endemic persistence alters prey-predator interactions by reducing healthy prey availability and shifting predator foraging pressure, thereby creating population baselines that resist simple ecological restoration.

Infection also reshapes long-term equilibria, with infected classes persisting at higher or more stable levels than healthy populations after transient dynamics. This disease-driven restructuring supports the conclusions of White et al. (2018) that parasite systems often settle into changed endemic baselines rather than returning to disease-free equilibria. From a control perspective, these results contextualize the vaccinomic strategies proposed by Rendón-Marín and Ruíz-Saenz (2024), suggesting that immunity-based interventions alone may be insufficient unless ecological transmission pathways particularly those mediated by predation are simultaneously addressed.

The transition from regular limit cycles in disease-free systems to more complex and irregular phase-space trajectories following disease introduction reflects strong non-linear feedbacks between predation and infection. This behavior reflects the challenges highlighted by White et al. (2018) in predicting wildlife disease dynamics and contrasts with the relatively predictable results of deterministic prey-predator models such as that examined by Stephano and Jung (2021). These findings confirm that deterministic models are insufficient for capturing disease-driven instability under environmental uncertainty and that coupled stochastic ecological models are necessary to assess system stability accurately.

Correlation analyses further reveal that disease status reshapes interaction strengths, producing weak or negative associations among population classes and near independence between predator health states. These patterns are consistent with the spatial and genetic heterogeneity in CDV host dynamics reported by Wipf et al. (2025) and support broader host-diversity insights documented in empirical CDV studies. Such interaction structures emphasize the importance of explicitly incorporating transmission pathways and stochastic perturbations, as random effects can alter correlations and stabilize or destabilize outbreaks.

Therefore, the findings demonstrate that the combined effects of stochasticity, predation, and disease transmission fundamentally reshape prey-predator dynamics. Environmental variability amplifies fluctuations, sustains endemic infection, and alters long-term equilibria, while nonlinear disease feedbacks generate complex and less predictable behavior. These results align with and previous studies on CDV persistence and wildlife disease heterogeneity, focusing that robust assessment of disease risk and extinction requires integrated ecological and epidemiological modeling under stochastic influences.

Conclusion

This study investigates the complex interplay between predation, disease, and environmental variability within a prey-predator ecosystem. Using a deterministic model coupled with Monte Carlo simulations. The results reveal that while classical prey-predator cycles provide the baseline for population dynamics, the introduction of disease and randomness fundamentally reshapes ecosystem behavior. Populations initially display oscillations characteristic of prey-predator interactions; however, infection modifies these dynamics by reducing prey quality and predator viability, thereby weakening trophic linkages. Over time, fluctuations tend to stabilize into a dynamic equilibrium, but this equilibrium deviates significantly from the patterns predicted by purely deterministic models. Disease acts as both a stabilizing and destabilizing properties, while predation suppresses prey abundance and can help limit infection spread, infected prey can also serve as reservoirs that sustain pathogen persistence and expose predators to additional risks. Environmental variability further amplifies this interplay, introducing irregularities and nonlinear feedbacks that make species interactions unpredictable. Phase-space visualizations confirm that disease increases ecological complexity, fragmenting stable cycles into asymmetric, dispersed, and sometimes chaotic trajectories, particularly when both prey and predator populations harbor infection. Weak to moderate correlations among population groups highlight that infection status alters traditional ecological linkages, diminishing the strength of predator dependence on prey and disrupting classical energy transfer pathways. Therefore, the results emphasize that predation and disease are tightly coupled drivers of ecosystem dynamics. Their interaction governs short-term oscillations, long-term coexistence, and the likelihood of disease endemicity. By modifying both ecological and epidemiological processes, they reshape resilience, extinction risk, and persistence outcomes. These results emphasize the necessity of incorporating both trophic interactions and infection dynamics together with

stochastic influences into ecological models to capture the true complexity of natural systems.

Acknowledgements

The author sincerely thanks the Mkwawa University College of Education for the learning environment and supportive working conditions.

References

Chen W, An W, Gao Q, Bai J, Li H, Tang S and Yang M 2025 Calculation of COVID-19 disease burden using Monte Carlo simulation with dynamic disability weights and analysis of transmission characteristics. *BMC Public Health* 25(1): 2041.

Clancy D and Tjia E 2018 Approximating time to extinction for endemic infection models. *Math. Comput. Appl. Probab*. 20(4): 1043-1067.

De Risio L and Platt S 2014 Structural epilepsy. Canine and feline epilepsy*: J. Clin. Diagn. Manag. Wallingford: CABI*, 101-6.

Deem SL, Spelman LH, Yates RA and Montali RJ 2000 Canine distemper in terrestrial carnivores: a review. *J. Zoo Wildl. Med*. 31(4): 441-451.

Dorn MW, and Barnes CL 2022 Time-varying predation as a modifier of constant natural mortality for Gulf of Alaska walleye pollock. *Fish. Res.* 254: 106391.

Hayes BH, Vergne T, Andraud M and Rose N 2023 Mathematical modeling at the livestock-wildlife interface: scoping review of drivers of disease transmission between species. *Front. Vet. Sci*. *10*, 1225446.

Hayward MW, O'Brien J, and Kerley GI 2007 Carrying capacity of large African predators: predictions and tests. *Biol. Conserv.* 139(1-2): 219-229.

Martinez-Gutierrez M and Ruiz-Saenz J 2016 Diversity of susceptible hosts in canine distemper virus infection: a systematic review and data synthesis. *BMC Vet. Res*, 12(1): 78.

Naveenkumar V, Porteen K, Bharathi MV and Nag BP 2020 Deadly Canine Distemper: A Global Multispecies Disease. *Environ. Technol. Eng. Tech.* (pp. 225-245). Apple Academic Press.

Niewiesk S and Oglesbee M 2022 Paramyxoviridae, Pneumoviridae, Filoviridae, and Bornaviridae. *Vet. Microbiol.* 596-608.

Pomeroy-Arthur UE 2023 Morbillivirus infections in animal hosts of the Serengeti District of Northern Tanzania: PPRV and CDV in multi-host livestock communities, and CDV in African wild dogs (*Lycaon pictus)*. Doctoral dissertation, University of Glasgow.

Rendon-Marin S and Ruíz-Saenz J 2024 Universal peptide-based potential vaccine design against canine distemper virus (CDV) using a vaccinomic approach. *Sci. Rep. 14*(1), 16605.

Sadiq BA 2025 Modeling the Evolution of Population Dynamics Using Ordinary Differential Equations: Mathematical Analysis and Modern Applications. *CAJMTCS 6*(3), 303-3

Santoro B, Larese Filon F and Milotti E 2024 An Easy-to-Use Tool to Predict SARS-CoV-2 Risk of Infection in Closed Settings: Validation with the Use of an Individual-Based Monte Carlo Simulation. *Microorganisms*, *12*(12), 2401.

Shetty BR, Pai BJ, Salmataj SA and Naik N 2024 Assessment of Carcinogenic and non-carcinogenic risk indices of heavy metal exposure in different age groups using Monte Carlo Simulation Approach. *Sci. Rep. 14*(1), 30319.

Stephano MA and Jung IH 2021 Effects of refuge prey on stability of the prey-predator model subject to immigrants: A mathematical modelling approach. *Tanz. J. Sci. 47*(4), 1376-1391.

Stephano MA, Mayengo MM, Irunde JI and Kuznetsov D 2023 Sensitivity analysis and parameters estimation for the transmission of lymphatic filariasis. *Heliyon*, *9*(9).

Stephano MA, Irunde JI, Mayengo MM and Kuznetsov D 2024 The significance of stochastic CTMC over deterministic model in understanding the dynamics of lymphatic filariasis with asymptomatic carriers. *J. Appl. Math.* 2024(1): 2130429.

Sykes JE and Vandevelde M 2021 Canine distemper virus infection. In *Greene's Infectious Diseases of the Dog and Cat* (pp. 271-288). WB Saunders.

Valdez A, Sun H, Weiss HH and Aranson I 2025 Biomechanical modeling of spatiotemporal bacteria-phage competition. *Commun. Phys. 8*(1), 1-10.

Viana M, Cleaveland S, Matthiopoulos J, Halliday JO, Packer C, Craft ME and Lembo T 2015 Dynamics of a morbillivirus at the domestic–wildlife interface: Canine distemper virus in domestic dogs and lions. *Proc. Natl. Acad. Sci.* 112(5): 1464-1469.

White LA, Forester JD and Craft ME 2018 Dynamic, spatial models of parasite transmission in wildlife: Their structure, applications and remaining challenges. *J. Anim. Ecol.* 87(3): 559-580.

Wipf A, Perez-Cutillas P, Ortega N, Huertas-López A, Martínez-Carrasco C and Candela MG 2025 Geographical Distribution of Carnivore Hosts and Genotypes of Canine Distemper Virus (CDV) Worldwide: A Scoping Review and Spatial Meta-Analysis. *Transbound. Emerg. Dis.* 2025(1): 6632068.

Yan AW, Cao P and McCaw JM 2016 On the extinction probability in models of within-host infection: the role of latency and immunity. *J. Math. Biol.* 73(4): 787-813.